High-Yield Purification Process of Singlewalled Carbon Nanotubes

Jeong-Mi Moon, Kay Hyeok An, and Young Hee Lee*

Department of Physics, Institute of Basic Science, Sungkyunkwan University, Suwon 440-746, Republic of Korea

Young Soo Park and Dong Jae Bae

Department of Semiconductor Science and Technology and Semiconductor Physics Research Center, Jeonbuk National University, Jeonju 561-756, Republic of Korea

Gyeong-Su Park

Analytical Engineering Laboratory, Samsung Advanced Institute of Technology, Suwon 440-600, Republic of Korea

Received: January 22, 2001; In Final Form: March 20, 2001

Reproducible high-yield purification process of singlewalled carbon nanotubes was developed by combining two-step processes of thermal annealing in air and acid treatment. The process involves the thermal annealing in air with the powders rotated at temperatures of 470 °C for 50 min, which burns out the carbonaceous particles, and an acid treatment with HCl for 24 h, which etches away the catalytic metals. Control of the annealing temperature and rotation of the sample are crucial for high yield. Our reproducible optimal purification process provides a total yield of about 25 ∼ 30 wt % with less than 1 wt % of transition metals, which was confirmed by the thermogravimetric analysis. Bundling and length control depending on the different acid treatments will be further discussed.

Introduction

Carbon nanotubes (CNTs) with superb electronic, mechanical, and structural characteristics[1−3] provide strong applicabilities to new functional devices, for instance, field emission displays,[4−6] nanoscale transistors,[7,8] supercapacitors,[9−11] secondary batteries,[12−14] and various composites.[15,16] Traditionally, arc discharge was used for mass production.[17−19] More recently, laser vaporization technique provided relatively highly purified singlewalled CNTs (SWCNTs).[20] Most approaches in general produce powders containing not only CNTs but also other carbonaceous particles such as amorphous carbons, fullerenes, nanocrystalline graphites, and transition metals that were introduced as a catalyst during the synthesis.[17−23] This sometimes hinders an accurate analysis of CNT characteristics and limits the best performance of the CNT applications to new functional devices.

Several attempts have been tried to purify the CNT powders. Gas phase reaction or thermal annealing in air or oxygen atmosphere has been attempted, although the yield of final product was relatively low.[24,25] The key idea with these approaches is a selective oxidative etching processs, based on the fact that the etching rate of amorphous carbons is faster than that of CNTs. Since the edge of the CNTs can be etched away as well as carbonaceous particles during the annealing, it is crucial to have a keen control of annealing temperatures and annealing times to obtain high yield, although the yield is also dependent on the purity of the original sample. Liquid-phase reaction in various acids has been tried to remove the transition metals.[23,26,27] This process involves repeated steps of filterings and sonications in acidic solution, where the transition metals were melted into the solution. CNTs are usually cut into small lengths and sometimes broken completely. The remaining walls are severely damaged with strong acid solution, although the wall structures could be recovered by the subsequent annealing. Therefore, the choice of acids, the immersing time, and temperature are the key factors to have high yield, while maintaining the complete wall of CNTs. These two processes are complementary to each other to remove the carbonaceous particles and transition metals.

In this paper, we adopt these two purification steps to SWCNTs synthesized by catalytic arc discharge. Special care is taken to have high yield during the annealing process and acid treatment. The whole processes are reproducible and completely robust for mass production. The total yield of 25 ∼ 30 wt % was easily obtained with the metal content of less than 1 wt %.

Experimental Section

SWCNTs were prepared by conventional catalytic arc discharge.[28] The chamber was pumped out to a base pressure of 100 mTorr, and then the helium gas was introduced until the pressure reached 100 Torr. The total amount of catalyst in a graphite powder was fixed to be 5 wt %, with the ratio of the transition metals (Ni/Co/FeS = 1:1:1), where sulfur was added as a promotor.[28] This increased significantly the yield of CNTs deposited in the chamber. The systematic purification procedure is as follows. Since there is a chance that the raw samples may differ slightly from batch to batch, several batches were mixed together to increase the reproducibility of the original raw samples. The raw sample contains carbonaceous particles and transition metals. This cloth-like raw sample was grinded mechanically and transferred to the heating chamber, where the

* To whom correspondence should be addressed. E-mail: leeyoung@yurim.skku.ac.kr.

10.1021/jp0102365 CCC: $20.00
Published on Web 05/26/2001

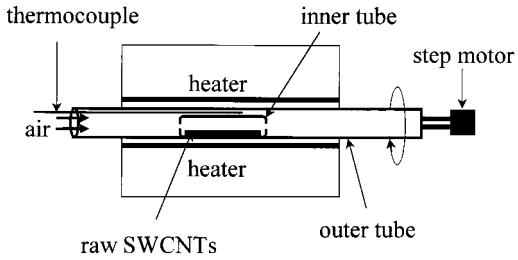

Figure 1. Schematic diagram of the apparatus used for thermal annealing process.

CNT powder was heated at 470 °C for 50 min in air to remove carbonaceous particles. We designed the heating apparatus,[29] where two quartz tubes were used, as can be seen in Figure 1. The inner tube contained the raw sample was rotated by the outer tube that was connected to a step motor with the rate of 30 rpm during the oxidation process, such that samples were evenly exposed to the surface to have uniformly selective etching by different oxidation rates controlled exclusively by the annealing time.

To remove the catalysts, the annealed powder was immersed and filtered in 6 M hydrochloric acid (HCl) for various times. This process was repeated several times until the color of acid was unchanged. The sample was finally washed out in deionized water. To unbundle SWCNTs, the sample obtained at the last step was sometimes boiled in 30% nitric acid (HNO_3) for 4−6 h. The obtained suspension was filtered with a PTFE (poly-(tetrafluoroethylene)) membrane in deionized water. After rinsing and drying the sample, a grayish black, thin mat composed of SWCNTs was finally obtained.

The morphology of SWCNTs and the degree of purification were observed by scanning electron microscope (SEM, Hitachi, S4700) and transmission electron microscope (TEM, Hitachi, H-9000NA). Fourier Transform (FT) Raman spectroscopy (BRUKER, RFS 100/S) using a Nd:YAG laser (1064 nm) was used to confirm the formation of graphitized carbon nanotubes and to investigate qualitatively the degree of purification. The total amount of residual metals in the samples was estimated using the thermogravimetric analysis (TGA, TA instruments, TGA 2950).

Results and Discussion

Morphology Characterization. Figure 2a shows a SEM image of the grinded raw soot collected from the whole chamber. In addition to the bundle of SWCNTs, the white spot, carbonaceous particles, mainly amorphous carbons, are shown in the figure. These structural features might be caused by variations in the arcing process because of an inhomogeneous distribution of catalysts in the anodes.[27] Furthermore, we can see that the metal particles were mainly embedded in larger amorphous carbons, as evidenced in Figure 3a.

This sample was thermally annealed at 470 °C for 50 min in air to remove selectively the amorphous carbons. The SEM image of oxidized SWCNTs is shown in Figure 2b. The figure shows a dramatic decrease of amorphous carbons after oxidation. As a result of oxidation, the weight of the soot was reduced to about 40 wt % of the original sample. The basic idea of the selective etching is that amorphous carbons can be etched away more easily than SWCNTs due to the faster oxidation reaction

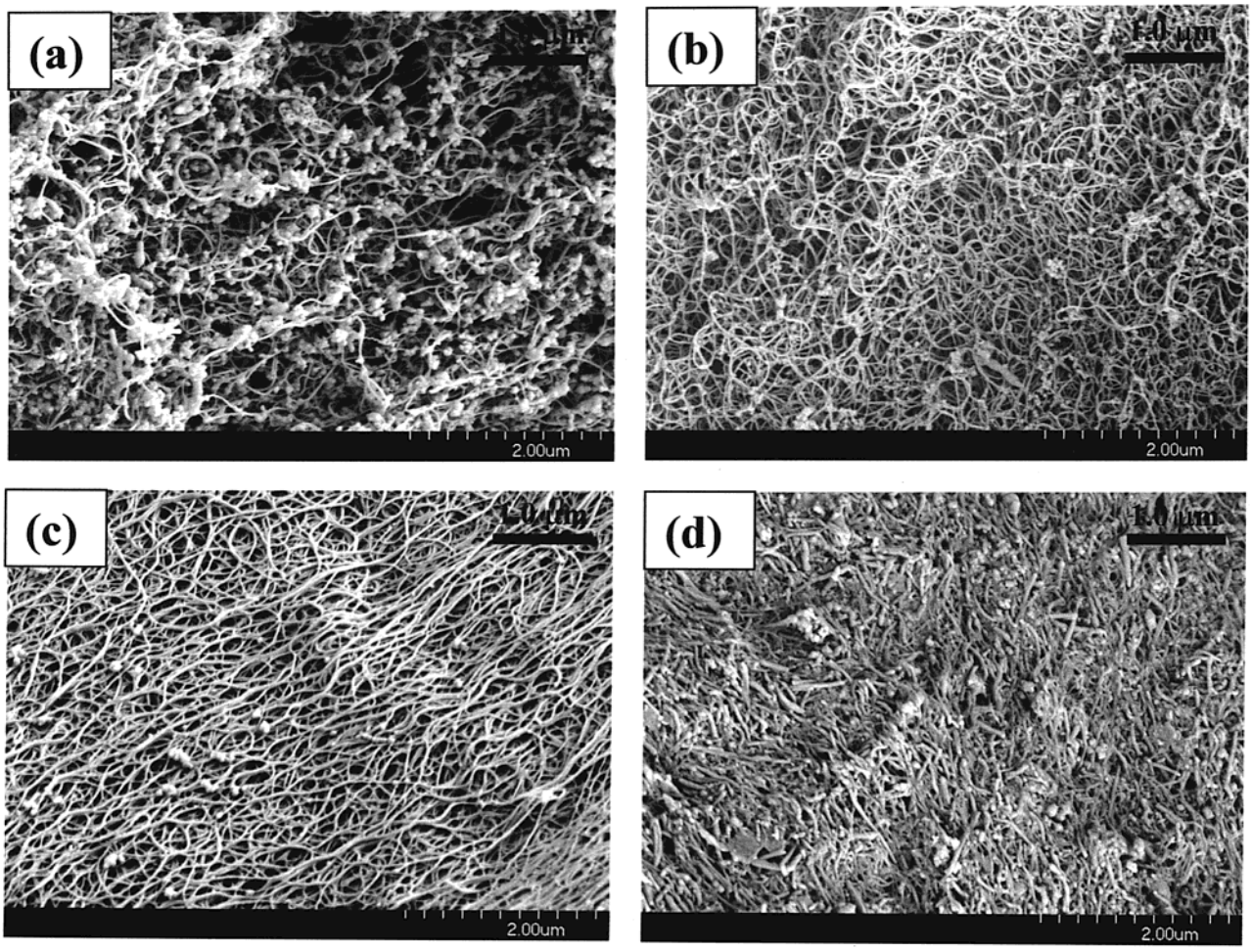

Figure 2. SEM images of (a) the raw SWCNT sample, (b) the thermally treated sample, (c) HCl-treated sample, and (d) HNO_3-treated sample.

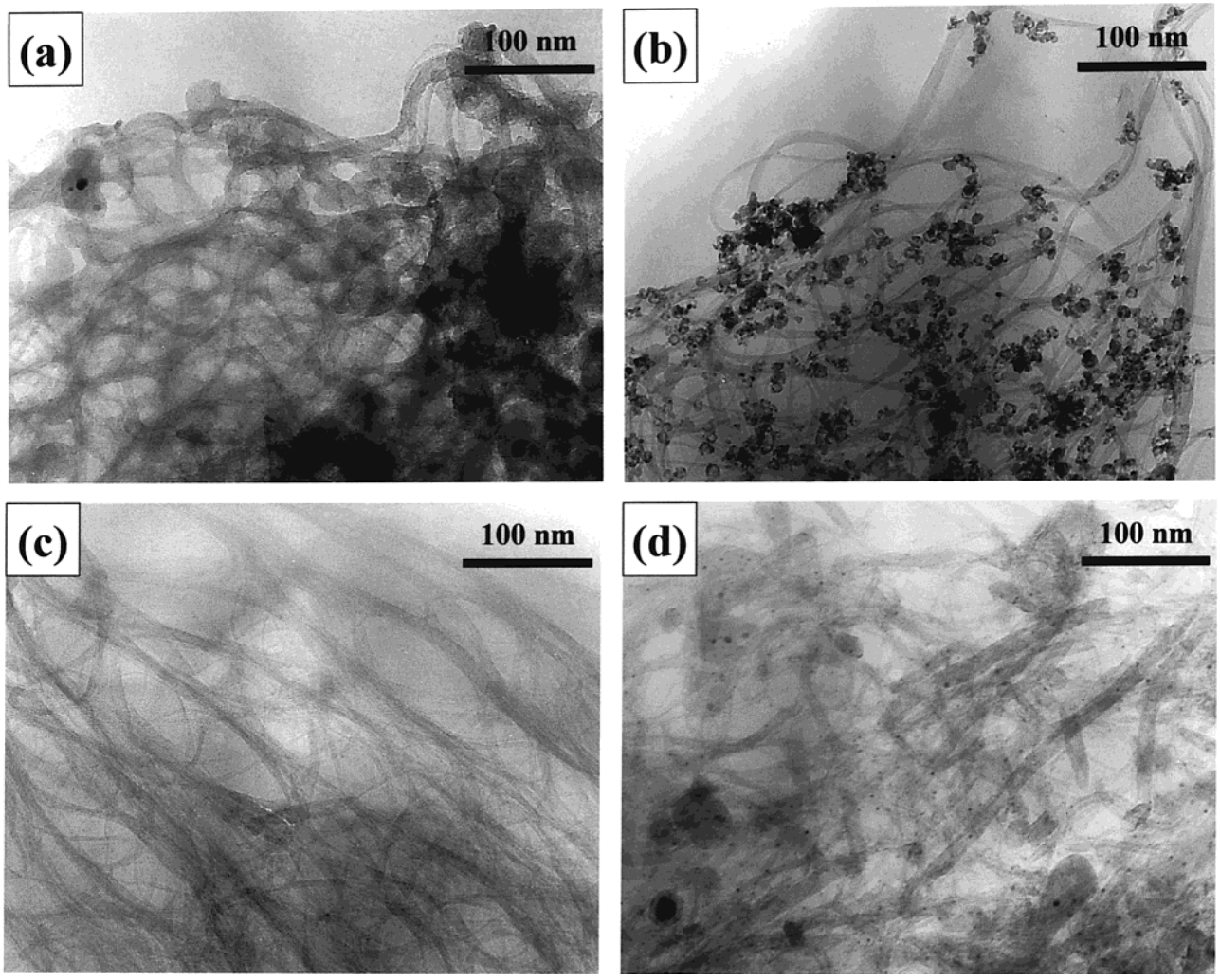

Figure 3. TEM images of (a) the raw SWCNT sample, (b) the thermally treated sample, (c) HCl-treated sample, and (d) HNO_3-treated sample.

rates.[30] Since the CNTs are etched away at the same time, the yield is usually low. For instance, Ebbesen et al. obtained only 1 wt % of the original sample after annealing in air at 750 °C for 30 min.[24] Thus, control of temperatures and annealing times is of crucial importance for high yield of CNTs. Furthermore, an even exposure of all parts of the CNTs to the oxidative species enhances the yield of the thermal treatment. This was achieved by rotating the quartz tube that contains CNT powders using the step motor, as described before. The TEM image of the oxidized SWCNTs shown in Figure 3b suggests that amorphous carbons coated on the surfaces of SWCNT bundles and those surrounding the catalytic metals were removed. Now the transition metals, as indicated by the black spots in Figure 3b, are left. We also tried several different annealing temperatures and times. The yield was very poor at temperatures greater than 500 °C. Too long annealing times were required at temperatures less than 450 °C. However, we note that this temperature is strongly catalyst-dependent. For instance, our optimum temperature is 470 °C, whereas the same arc discharge with different catalysts (Y, Ni) gave the evaporation temperature of 350 °C.[23] This effect will be discussed later.

The transition metals can be etched away by an acid treatment. Figure 2c shows the SEM image of the acid-treated sample, where the annealed sample was immersed in 6 M hydrochloric acid for 24 h. The corresponding TEM image in Figure 3c clearly shows that the transition metal particles were well melted away. Yet some carbonaceous particles, which are left during the annealing procedure, still remain in the sample, as illustrated in Figure 2c. Special care should be taken to obtain better purified samples. We note that the acid treatment enhances the bundling of SWCNTs, as shown in Figure 2c, as compared to the annealed samples in Figure 2b, since the entangled SWCNTs are released in acid and aggregated themselves by the van der Waals interactions. This acid treatment gave the yield of 70 wt % of the thermally annealed samples. Thus, the total yield of two steps is about 25 $\sim$ 30 wt %. To disperse the CNT bundles, the above samples were again boiled in nitric acid for 6 h. Some opaque backgrounds represent the well-dispersed SWCNTs, although SWCNTs were broken into small pieces, as shown in Figure 2d. It is interesting to observe some multiwalled CNTs, as shown in Figure 3d. These were formed during the nitric acid treatment. Disintegration of some SWCNTs in the bundle may occur during the acid treatment. For instance, some unzipping of SWCNTs can be promoted in the presence of hydrogen and oxygen atoms.[31] Yet, the origin of such a formation mechanism is not clear at this moment.

Resonant Raman Scattering Spectra. Raman spectroscopy was employed to identify changes of the raw and purified samples. Figure 4 shows typical Raman spectra for single-walled carbon nanotubes, the Raman spectra of SWCNTs have fingerprint features, which is quite different from those of graphite, multiwalled carbon nanotubes, and amorphous carbon. The spectra are composed of two characteristic zones. The first zone consists of high frequency with maximum intensity near

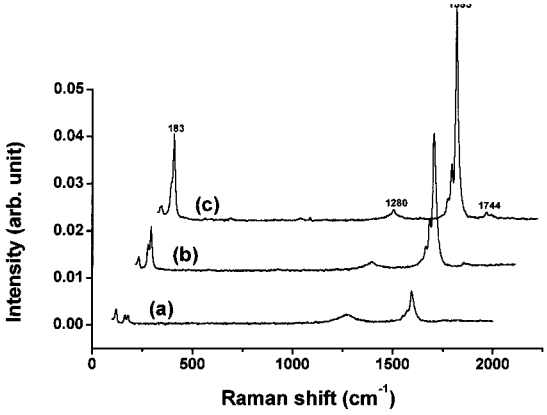

Figure 4. FT-Raman spectra of (a) the raw SWCNT sample, (b) the thermally treated sample, and (c) HCl-treated sample.

1593 cm^{-1}, so-called tangential modes, which are related to the graphite E_{2g} symmetry intralayer mode, split due to the curvature of the rolled-up graphite sheet.[32] The high-frequency bands of the raw (shown in Figure 4a) and the purified (Figure 4b,c) carbon nanotubes exhibit similar band positions which be decomposed into three peaks at 1593, 1571, and 1552 cm^{-1}. The Raman spectra of MWCNTs and graphite exhibit only a single peak at 1583 cm^{-1}.[29]

The second zone, in the low-frequency range of 160 ~ 200 cm^{-1}, consists of the radial breathing modes (RBM) whose frequencies depend on the tube diameters.[33] This is also a characteristic of SWCNTs, since MWCNTs do not show any low-frequency mode and the low-frequency mode of graphite is at 42 cm^{-1}. A broad band is usually observed around 1280 cm^{-1} in graphite and multiwall tubes,[29,34,35] which is a characteristic of amorphous carbon or defects, and is also observed in Figure 4. After the purification, the intensity of the peak at 1280 cm^{-1} is decreased, whereas the intensities of near the peak at 1593 and 183 cm^{-1} are increased drastically. The intensity ratio of the 1593 cm^{-1} peak to 1280 cm^{-1} peak gradually increases for annealed samples. This ratio is even greater in acid-treated sample, which may indicate the dense samples formed after acid treatment. It is of note that the second-order Raman peak near 1744 cm^{-1} is developed in the purified samples, which is another indicative of the degree of purification.

Thermogravimetric Analysis. Figure 5 shows the TGA graphs and the differentiated TGAs of the raw soot and the purified SWCNTs. In the raw sample, as shown in Figure 5a, the weight starts reducing near 300 °C. This temperature is relatively low but presumably catalyst-assisted dissociation takes place during the process. The SWCNTs are completely evaporated near 900 °C. The remaining materials are the transition metals, which is about 8 wt %. The differentiated TGA demonstrates the existence of at least three phases in the sample. One phase that shows a broad peak position at 500 °C is assumed to be amorphous carbons, although a small peak appears near 550 °C, which may be conjectured as crystalline nanoparticles. Another phase at 800 °C is the SWCNTs. The larger integrated area of the first and second peaks as compared to the third one indicates that more carbonaceous particles than SWCNTs in fact exist in the sample, reflecting the yield of our powder. Our choice of the annealing temperature at 470 °C seems to be reasonable from this analysis. We note that the evaporation temperature may vary with different compositions of catalysts. The evaporation temperature of our sample is greater than the previously reported one.[23] The TGA of the annealed samples in Figure 5b shows relatively a simple monotonic decrease with increasing temperatures. The amorphous carbons are mostly removed, although a small amount of amorphous carbons still remain in the sample, as indicated by the small peak from the differentiated TGA curve near 400 °C. The remaining metal content is high in this case (18 wt %), as expected from the relative composition. Figure 5c shows that the transition metals are nearly melted away to the TGA detection limit (<1 wt %) for acid-treated sample after the thermal treatment. The differentiated TGA peak is narrower, indicating mostly evaporation of SWCNTs. Yet, a small bump near 550 °C exists, suggesting that carbonaceous particles still

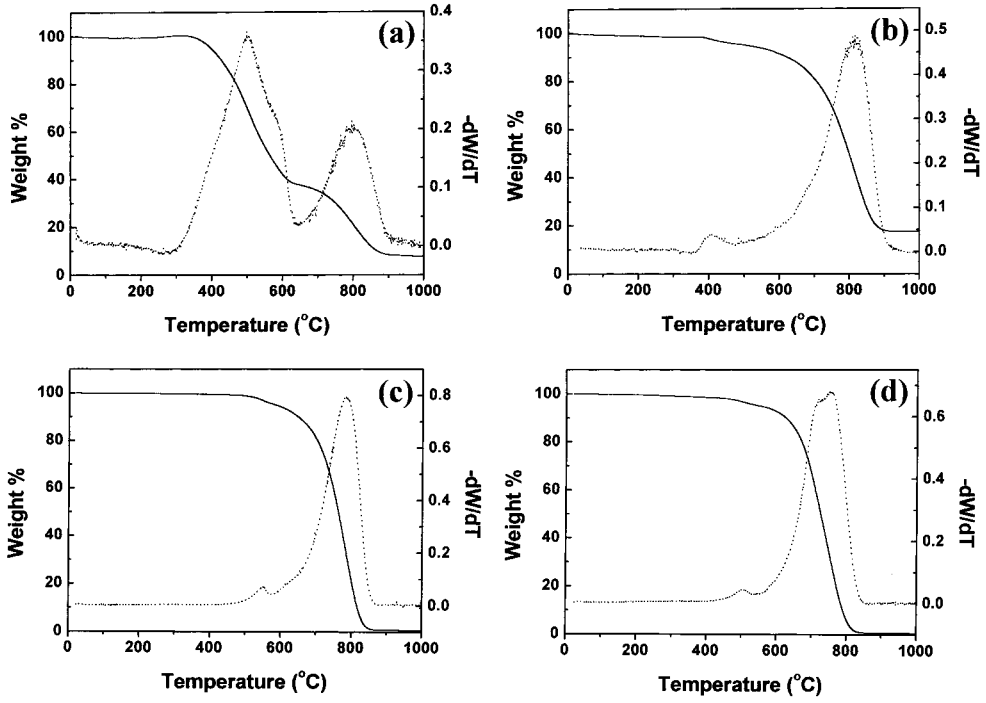

Figure 5. TGA graphs of (a) the raw SWCNT sample, (b) the thermally treated sample, (c) HCl-treated sample, and (d) HNO_3-treated sample. The solid and dot lines correspond to the TG and differentiated TG curves, respectively.

remain in the sample. The estimated purity of the sample from the integrated area of the differentiated TGA is about 96 wt %. After the nitric acid treatment (Figure 5d), the CNT peaks are separated, indicating some other new phases are created, as suggested in the TEM images.

Conclusion

We have obtained high-yield SWCNTs by combining two-step processes of thermal annealing in air and acid treatment. The optimal conditions are the thermal annealing in air with the powders to be rotated at temperatures of 470 °C for 50 min and HCl acid treatment for 24 h. Our reproducible optimal purification process provides a total yield of about 25−30 wt % with less than 1 wt % of transition metals and 96 wt % of purity, which was confirmed by the thermogravimetric analysis. Longer thermal treatment will results in better purity but lower yield. We also find that nitric acid treatment breaks down the CNTs into small pieces and sometimes forms multiwalled CNTs.

Acknowledgment. This work was supported in part by the Ministry of Science and Technology (MOST) through National Research Laboratory (NRL) and New Frontier programs and in part by the Brain Korea 21 (BK21) program.

References and Notes

(1) Caroll, D. L.; Redlich, P.; Ajayan, P. M.; Charlier, J. C.; Blase, X.; de Vita, A.; Car, R. *Phys. Rev. Lett.* **1997**, *78*, 2811.
(2) Wong, E. W.; Shennah, P. E.; Lieber, C. M. *Science* **1997**, *277*, 1971.
(3) Cahill, P. A.; Rohlfing, C. M. *Tetrahedron* **1996**, *52*, 5247.
(4) Fan, S.; Chapline, M. G.; Franklin, N. F.; Tombler, T. W.; Cassel, A. M.; Die, H. *Science* **1999**, *283*, 512.
(5) Collins, P. G.; Zettle, A. *Phys. Rev. B* **1997**, *55*, 9391.
(6) Bonard, J.-M.; Salvetat, J. P.; Stockli, T.; de Heer, W. A.; Forro, L.; Chatelain, A. *Appl. Phys. Lett.* **1998**, *73*, 918.
(7) Tans, S. J.; Verschueren, R. M.; Dekker, C. *Nature* **1997**, *386*, 474.
(8) Tans, S. J.; Verschueren, R. M.; Dekker, C. *Nature* **1998**, *393*, 49.
(9) Niu, C.; Sichel, E. K.; Hoch, R.; Moy, D.; Tennent, H. *Appl. Phys. Lett.* **1997**, *70*, 1480.
(10) Diederich, L.; Barborini, E.; Piseri, P.; Podesta, A.; Milani, P.; Schneuwly, A.; Gallay, R. *Appl. Phys. Lett.* **1999**, *75*, 2662.
(11) An, K. H.; Kim, W. S.; Park, Y. S.; Choi, Y. C.; Lee, S. M.; Chung, D. C.; Bae, D. J.; Lim, S. C.; Lee, Y. H. *Adv. Mater.* **2001**, *13*, 497.
(12) Wu, G. T.; Wang, C. S.; Zhang, X. B.; Yang, H. S.; Qi, Z. F.; He, P. M.; Li, W. Z. *J. Electrochem. Soc.* **1999**, *146*, 1696.
(13) Frackowiak, E.; Gautier, S.; Gaucher, H.; Bonnamy, S.; Beguin, F. *Carbon* **1999**, *37*, 61.
(14) Lee, S. M.; Park, K. S.; Choi, Y. C.; Park, Y. S.; Bok, J. M.; Bae, D. J.; Nahm, K. S.; Choi, Y. G.; Yu, S. C.; Kim, N. G.; Frauennnheim, T.; Lee, Y. H. *Synth. Metals* **2000**, *113*, 209.
(15) Ajayan, P. M.; Schadler, L. S.; Giannaris, C.; Rubio, A. *Adv. Mater.* **2000**, *12*, 750.
(16) Flahaut, E.; Peigney, A.; Laurent, Ch.; Marlière, Ch.; Chastel, F.; Rousset, A. *Acta Mater.* **2000**, *48*, 3803.
(17) Journet, C.; Maser, W. K.; Bernier, P.; Loiseau, A.; de la Chapelle, M. L.; Lefrant, S.; Deniard, P.; Lee, R.; Fischer, J. E. *Nature* **1997**, *388*, 756.
(18) Saito, Y.; Tani, Y.; Miyagawa, N.; Mitsushima, K.; Kasuya, A.; Nishina, Y. *Chem. Phys. Lett.* **1998**, *294*, 593.
(19) Shi, Z. J.; Lian, Y. F.; Zhou, X. H.; Gu, Z. N.; Zhang, Y.; Iijima, S.; Zhou, L. X.; Yue, K. T.; Zhang, S. L. *Carbon* **1999**, *37*, 1449.
(20) Thess, A.; Lee, R.; Nikolaev, P.; Dai, H.; Petit, P.; Robert, J.; Xu, C.; Lee, Y. H.; Kim, S. G.; Rinzler, A. G.; Colbert, D. T.; Scuscria, G. E.; Tománek, D.; Fischer, J. E.; Smally, R. E. *Science* **1996**, *273*, 483.
(21) Kataura, H.; Kumazawa, Y.; Maniwa, Y.; Umezu, I.; Suzuki, S.; Ohtsuka, Y.; Achiba, Y. *Synth. Met.* **1999**, *103*, 2555.
(22) Flahaut, F.; Govindaraj, A.; Peigney, A.; Laurent, C.; Rousset, A.; Rao, C. N. R. *Chem. Phys. Lett.* **1999**, *300*, 236.
(23) Shi, Z. J.; Lian, Y. F.; Liao, F. H.; Zhou, X. H.; Gu, Z. N.; Zhang, Y.; Iijima, S. *Solid State Commun.* **1999**, *112*, 35.
(24) Ebbesen, T. W.; Ajayan, P. M.; Hiura, H.; Tanigaki, K. *Nature* **1994**, *367*, 519.
(25) Zimmerman, J. L.; Bradley, R. K.; Huffman, C. B.; Hauge, R. H.; Margrave, J. L. *Chem. Mater.* **2000**, *12*, 1361.
(26) Tohji, K.; Takahashi, H.; Shinoda, Y.; Shimizu, N.; Jeyadevan, B.; Matsuoka, I.; Saito, Y.; Kasuya, A.; Ito, S.; Nishina, Y. *J. Phys. Chem. B* **1997**, *101*, 1974.
(27) Liu, B.; Wågberg, T.; Olssen, E.; Yang, R.; Li, H.; Zhang, S.; Yang, H.; Zou, G.; Sundqvist, B. *Chem. Phys. Lett.* **2000**, *320*, 365.
(28) Park, Y. S.; Kim, K. S.; Jeong, H. J.; Kim, W. S.; Moon, J.-M.; An, K. H.; Bae, D. J.; Lee, Y. S.; Park, G.-S.; Lee, Y. H. *Synth. Met.*, submitted for publication.
(29) Park, Y. S.; Choi, Y. C.; Kim, K. S.; Chung, D.-C.; Bae, D. J.; An, K. H.; Lim, S. C.; Zhu, X. Y.; Lee, Y. H. *Carbon* **2001**, *39*, 655.
(30) Zhu, X. Y.; Lee, S. M.; Lee, Y. H.; Frauenheim, T. *Phys. Rev. Lett.* **2000**, *85*, 2757.
(31) Lee, S. M.; Lee, Y. H., unpublished observations.
(32) Eklund, P. C.; Holden, J. M.; Jishi, R. A. *Carbon* **1995**, *33*, 959.
(33) Rao, A. M.; Bandow, S.; Richter, E.; Eklund, P. C. *Thin Solid Films* **1998**, *331*, 141.
(34) Hiura, H.; Ebbesen, T. W.; Tanigaki, K.; Takahashi, H. *Chem. Phys. Lett.* **1993**, *202*, 509.
(35) Li, W.; Zhang, H.; Wang, C.; Xu, L.; Zhu, K.; Xie, S. *Appl. Phys. Lett.* **1997**, *70*, 2684.